

Numerical Investigation of the Effect of Incoherence on Fast Wave Generation in Cancellous Bone

海綿骨中の高速波生成におけるインコヒーレンスの影響のシミュレーションによる検討

Yoshiki Nagatani^{1,3†}, Hirofumi Taki², Guillaume Haïat³, and Mami Matsukawa⁴
(¹Kobe City Coll. Tech.; ²Kyoto Univ.; ³CNRS, Laboratoire MSME UMR CNRS 8208 Créteil; ⁴Doshisha Univ.)

長谷 芳樹^{1,3†}, 瀧 宏文², ギヨーム・ハイアット³, 松川 真美⁴
(¹神戸市立工業高等専門学校, ²京都大学大学院, ³CNRS・パリ東大学クレティユ, ⁴同志社大学)

1. Background

Quantitative ultrasound (QUS) technique is now used in clinical practice for the assesment of bone strength [1,2]. For this purpose, an interesting behavior of pulse wave separation propagating in cancellous bone, refered to as *two wave phenomenon* [3], has been considered useful for precise estimation of not only bone density but also *bone quality* [4]

The frequency of the fast wave has been shown to be lower than that of the slow wave, which often lasts temporally longer depending on the condition of bone specimen [5-8]. The existence of two waves has been interpreted as the effect of their discriminating propagation paths: the fast wave mainly reflects the properties of the solid part (trabeculae) of cancellous bone and slow wave reflects that of liquid part (bone marrow) [4]. However, in some cases, the shape of the waveform of the received wave is collapsed because of the incoherence of propagating wave, and, as a result, it may be difficult to derive pertinent information of the media [9]. In this study, therefore, we investigated the effect of wave incoherence on the two waves properties propagating in heterogeneous cancellous bone using 3-D numerical simulation.

2. Simulation Setup

Three-dimensional elastic FDTD (finite-difference time-domain) simulations were performed using X-ray microcomputed tomography images of bovine cancellous bone specimens (see Fig. 1) [10]. The size of the specimens was $15 \times 15 \times 9 \text{ mm}^3$ and the spatial resolution of CT images and simulation was $46 \mu\text{m}$. With these specimens, it was confirmed that a clear separation of two waves could be observed.

In order to confirm the effect of the heterogeneity of specimen, three types of repetition models were artificially created.

As shown in Figs.2, the original model (Model-2) was separated into nine cuboids (Fig.2(a)), and then the each part was copied eight times using symmetry and mirrored images to avoid discontinuity (Fig.2(b)-(d)).

Then, a short ultrasonic pulse was applied into the aforementioned structures using a $15 \times 15 \text{ mm}^2$ planar transmitter. The emitted signal was chosen similar as a received wave acquired in similar measurement setup, with a 1 MHz single sinusoidal wave [10].

The size of simulation domain was $17 \times 17 \times 13 \text{ mm}^3$. The propagated waves were observed with planar receivers parallel to the transmitter. Here, coaxial square sensors with different sizes (from $46 \times 46 \mu\text{m}^2$ up to $15 \times 15 \text{ mm}^2$) were prepared in order to determine the effect of the summation of possible incoherent waves.

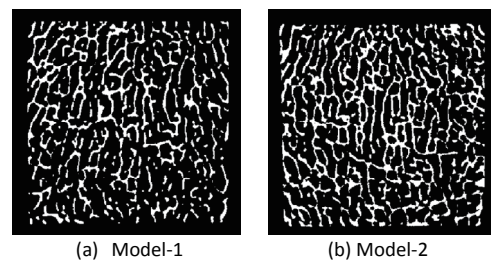
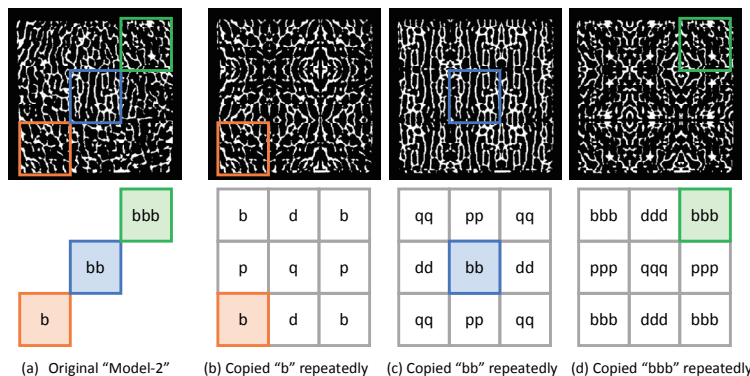


Fig.1 Cross-section diagrams (central slice) of 3-D simulation models: (a) Model-1 and (b) Model-2.



(a) Original "Model-2" (b) Copied "b" repeatedly (c) Copied "bb" repeatedly (d) Copied "bbb" repeatedly

Fig.2 Preparation of artificial repetition models based on Model-2 shown in Fig.1(b). (a) The original model was separated into 9 parts and then copied to (b) (c) (d) alternately as erecting images (e.g. $b \rightarrow b$) or mirrored images (e.g. $b \rightarrow d$, $b \rightarrow p$, or $b \rightarrow q$), respectively.

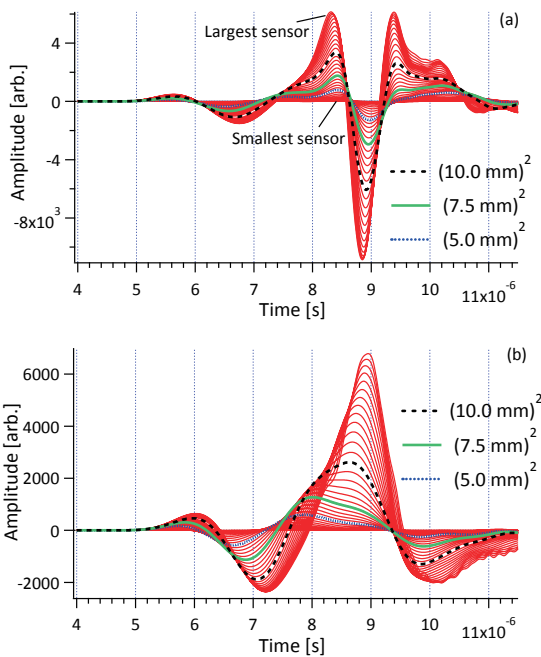


Fig.3 Simulated results of (a) Model-1, (b) Model-2. Each line indicates the result with various sensor size.

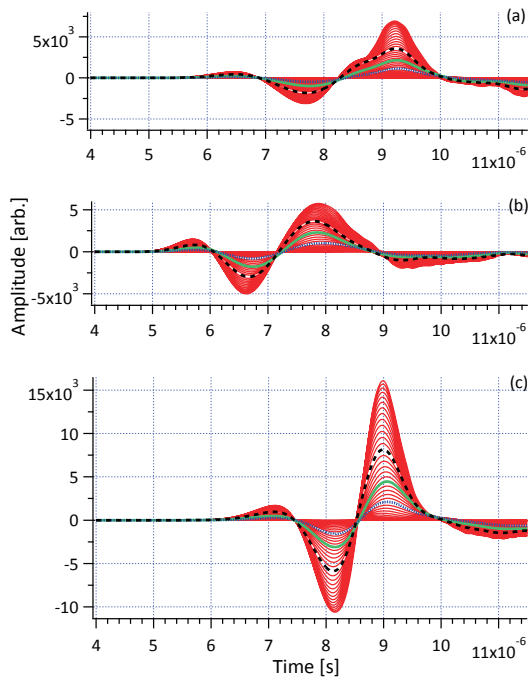


Fig.4 Simulated results of artificial repetition models based on Model-2 shown in Fig.2(b)-(d).

3. Results and Discussion

Figures 3 show the simulated waveforms received by each transducer with different sizes. For both models, fast waves and slow waves can be distinguished: the time of arrival of the fast wave is around 5.0~6.0 μs in (a) and 5.5~6.5 μs in (b), while the slow wave arrives at 8.0~9.0 μs in (a) and 7.5~9.5 μs in (b). In addition, the results of (a) show that the peak positions of fast and slow waves are almost independent of the sensor size, respectively.

In contrast, the peak positions of especially the slow waves in (b) are strongly dependent of the sensor size.

The results shown in **Figs.4** may help to understand the behavior of the times of flight of the fast and slow wave modes as a function of the transducer size. Figures 4(a), (b), and (c) show the results of the models corresponding to spatial repetitions. Each result only reflects the corresponding targeted area of the original model (Model-2 shown in Fig.1(b)), respectively. Figure 5 indicates that the peak positions of fast and slow waves strongly depend on the location of specimen and not on sensor size. Thus, considering the sensor size may be a good method to investigate the effect of the incoherence of the propagating wave in the case of heterogeneous bone samples.

4. Conclusion

The ultrasonic propagation in cancellous bone samples was simulated using the coupling of numerical simulation tools with high resolution imaging techniques. The peak positions of the fast and slow wave modes may be influenced by the sensor size, depending on the specimen properties. The results indicate that the sensor size is an important parameter which should be taken into account while performing clinical measurements because the received wave may be affected by the heterogeneous distribution of the microstructure of the specimen which may cause incoherence of the propagating wave.

Acknowledgment

This work was partly supported by JSPS KAKENHI Grant Number 25871038, 24360161, and 25870345.

References

1. NIH, J. Am. Med. Assoc., **285** (2001) 785.
2. P. Laugier and G. Haïat, ed.: *Bone Quantitative Ultrasound* (Springer, 2011).
3. A. Hosokawa and T. Otani: J. Acoust. Soc. Am. **101** (1997) 558.
4. G. Haïat, F. Padilla, M. Svrcekova, T. Chevalier, D. Pahr, P. Laugier, and P. Zysset: J. Biomech. **42** (2009) 2033.
5. G. Haïat, F. Padilla, F. Peyrin, and P. Laugier: J. Acoust. Soc. Am. **23** (2008) 1694.
6. L. Cardoso, F. Teboul, L. Sedel, C. Oddou, and A. Meunier: J. Bone Miner. Res. **18** (2003) 1803.
7. S. Hasegawa, Y. Nagatani, K. Mizuno, M. Matsukawa: Jpn. J. Appl. Phys. **49** (2010) 07HF28.
8. Y. Nagatani and R.O. Tachibana, J. Acoust. Soc. Am. **135** (2014) 1197.
9. F. Fujita, K. Mizuno, and M. Matsukawa: J. Acoust. Soc. Am., **134** (2013) 4775.
10. Y. Nagatani, K. Mizuno, and M. Matsukawa: Ultrasonics **54** (2014) 1245.